NRIAG JOURNAL OF ASTRONOMY AND GEOPHYSICS
2024, VOL. 13, NO. 1, 46–60
https://doi.org/10.1080/20909977.2024.2331902

Near surface resistivity investigation of regolith of Middle Benue Trough: implications on road pavement along Lafia-Shendam Axis, North Central Nigeria

Olawale Babatunde Olatinsu[a] and Yohanna Kigbu Abimiku[b]

[a]Department of Physics, University of Lagos, Lagos, Nigeria; [b]Nigerian Building and Road Research Institute, Skills Acquisition Center/ Pozzolana Pilot Plant, Bokkos, Plateau, Nigeria

ABSTRACT

Electrical characteristics and subsurface structures associated with the regolith of Middle Benue Trough have been investigated. Vertical electrical sounding (VES) and constant separation traversing (CST) techniques were employed for data acquisition along Lafia-Shendam Road, Lafia, North Central Nigeria. Forty (40) Schlumberger sounding stations and four (4) Wenner resistivity profiles were occupied along opposite sides of the road to delineate and decipher the subsurface geological structures. Second-order Dar Zarrouk parameters (longitudinal and transverse resistivities, mean resistivity and coefficient of anisotropy) computed from VES parameters were also used to evaluate the pseudo-anisotropy characteristics of the regolith cover. Geoelectric sequences delineated within the study area include thin topsoil, alluvium deposit, weathered layer (laterite and saprolite) and fresh basement. The regolith is hosted by a weathered sedimentary rock at an average depth which varies from 10.2 to 37.3 m. The regolith structure is not complex and has a greater proportion of conductive laterite. The saprolite associated with the host sedimentary rock, masked in the VES technique, is revealed as a very thin zone with moderate resistivity in the CST 2-D structures. The predominance of laterite in the regolith is also corroborated by the range of values of the coefficient of anisotropy and mean resistivity.

ARTICLE HISTORY
Received 25 October 2022
Revised 30 August 2023
Accepted 13 March 2024

KEYWORDS
Electrical resistivity; regolith; laterite; saprolite; basement rocks

1. Introduction

Road pavement stability and performance are more often discussed and evaluated based on pavement structure and design specifications. However, the nature, characteristics and competence of the native Earth material used as the subgrade can be a significant factor in the durability and longevity of pavements (Daud et al. 2019; Smaida et al. 2021; Vaiana et al. 2021). Incorporating geological and geophysical investigations into geotechnical works from the early stages of the planning and construction of roads and other infrastructures can contribute significantly **to** cost reduction, increased construction safety and avoidance of future perennial problems (Georgiadis et al. 2007). This implies that information on the subsurface geological condition at project site is important in the selection, design and construction of infrastructures (Okagbue and Uma 1988; Smith 1988). For roads and highways, the suitability and performance of a subgrade in geotechnical works depends substantially on its load bearing capacity and volume changes (Petry and Little 2002; Biggs and Mahony 2004; Rasul et al. 2016; Daud et al. 2019). Load bearing capacity is a function of several factors, such as the degree of compaction, moisture content, soil type, mineral content, etc. A good subgrade is a subsurface material that can support a large amount of loading without excessive deformation. Also, some soils undergo remarkable amount of volume change when exposed to excessive moisture or some fluctuating climatic and seasonal conditions. Some clay soils shrink and swell depending upon their moisture content, while soils with excessive fine grain constituents may be susceptible to frost heave in temperate regions (Jone 2017; Hobbs et al. 2019).

About 95% of the Earth's crust is covered with loose or unconsolidated Earth material from the exposed surface to some considerable depth (Hunt 1986). In the highly tropical to sub-tropical zones, the upper subsurface zones are mainly characterised by some regolith cover. Regolith occurs extensively both in the Precambrian shields, as well as in adjacent and overlying sedimentary basins in many countries in Africa (Ola, 1978, 1980; Omorinbola 1983; Agbede 1992; Key 1992; Kellett et al. 2004; Obiora 2006; Chardon et al. 2018). Much of this regolith is residual and consists of loose and unlithified soil materials (lateritic soils and clay-rich saprolites) which originate from intensely weathered bedrock and overlying components of transported material of varying degrees of weathering

CONTACT Olawale Babatunde Olatinsu oolatinsu@unilag.edu.ng Department of Physics, University of Lagos, Akoka, Yaba, Lagos, Nigeria

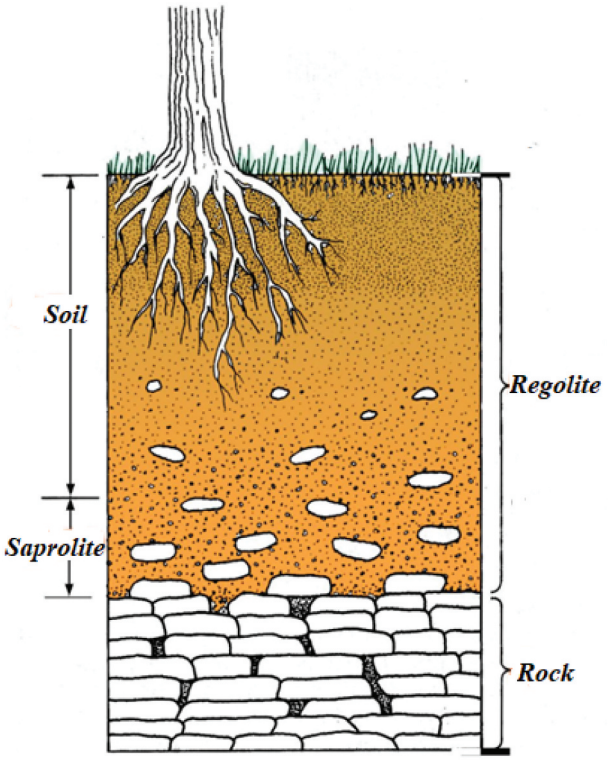

Figure 1. Typical subsurface sequence in a basement complex terrain showing regolith (soil, saprolite) overlying the fresh bedrock (adapted from Juilleret et al. 2014).

(Eggleton et al. 2008; Graham et al. 2010; Juilleret et al. 2014; Pedron et al. 2015). Generally, regolith extends from topsoil to the top of the fresh bedrock (Figure 1) and in most parts of Africa includes fractured and weathered basement rocks, saprolites, soils (laterite, sand, clay, etc.), organic accumulations, alluvium, evaporitic sediments, aeolian deposits and groundwater (Butt et al. 1997; Anand and Butt, 1988; Gupta et al. 2008; Graham et al. 2010; Anand 2016). Since regolith is a product of many different geological processes, its physical characteristics (resistivity, density, permeability, porosity, etc.) can be highly variable over short distances. Therefore, the characterisation of the physical properties of regolith is of utmost importance in many mining, exploration, engineering and environmental and agricultural investigations and projects (Bishop et al. 2001; Munday et al. 2001, 2004; Govindan 2015; Pawlik and Kasprzak 2018; Gourdol et al. 2021). In some engineering works, regolith must be removed in order to construct foundations on bedrock. In other cases, it is the regolith itself on which structures are anchored or which constitutes the source of material for embankments and other earthworks. In hydrogeophysical and environmental studies, regolith can also be a locally significant aquifer that yields groundwater relatively easily and inexpensively (Jones 1985; Acworth 1987; Hazell et al. 1988, 1992; Wright 1992; MacDonald and Calow 2009; MacDonald and Edmunds 2014). However, since regolith lies at the Earth's surface, aquifers in it are much more easily exposed to pollution than those in deeper artesian aquifers. Several economic natural resources and deposits such as minerals are buried within regolith across many geological environments (Taylor and Eggleton 2001).

Geotechnical geophysical investigation has proven very useful in the imaging and characterisation of shallow or near subsurface region of the Earth, typically to depths of about several hundred metres (Keller 1974; Reynolds 1998; Massarch 2000; Lowrie and Fichtner 2019). There has been growing interest in its broad applications in the built industry, majorly in the construction of engineering structures and infrastructures such as roads, bridges, dams, rails and houses (Adebisi et al. 2016; Camarero and Moreira 2017; Romero-Ruiz et al. 2019). Several non-invasive survey and mapping techniques that have been developed can provide cost-effective subsurface delineation and characterisation of geological deposits and other targets of interest. Some of its well-established potentials include differentiation between geologic zones horizontally and vertically, generation of 1-D cross-sections, 2-D maps at desired depths or 3-D images for easy virtualisation of subsurface conditions (Romero-Ruiz et al. 2019). Among the many geotechnical geophysical tools, electrical resistivity technique has wide spread applications because resistivity or its inverse, conductivity, is related to the actual geologic properties of Earth materials (Keller and Frischknecht 1996). In addition, among all the geophysical properties of subsurface materials, electrical resistivity is undoubtedly the most variable and depends on geological and petrophysical factors such as rock type, porosity, connectivity of pores, nature of the fluid and metallic content of the solid matrix (Palacky 1987).

The site for this present investigation is situated along the Lafia-Shendam Road, Northwest of Lafia, Nasarawa State. Lafia lies between latitude 8° 20′ and 8° 38′ N and longitude 6° 34′ and 7° 30′ E in north-central Nigeria (Chunwate et al. 2019). Lafia-Shendam Road is a major highway which connects Nasarawa and Plateau States in the northcentral region with Taraba and Bauchi states in the northeastern region of Nigeria. Some parts of this road had become deathtraps as criminal elements take advantage of its dilapidated condition to attack motorists almost on a daily basis. The journey between Lafia, the Nasarawa State capital and Shendam in Plateau State, which ordinarily should last for an hour, now takes about 4 hours due to the deplorable condition of the road. About 60 km of this road is characterised by deep potholes with some areas completely washed away (Figure 2). The road was constructed by the Federal Government of Nigeria in 1976. Since then, rehabilitation and maintenance have been carried on some segments of the road. The Nasarawa State office of the Federal Roads Maintenance Agency (FERMA) carried out several

Figure 2. Some sections of the Lafia-Shendam Road showing cracks and potholes on the road pavement.

maintenance works on the road in 1992, 2019 and 2021 (FERMA 2020). But at the time of this study, several portions of the road had dilapidated. The aim of this study is to investigate the structure and characteristics of regolith along Lafia-Shendam Road using vertical electrical sounding (1-D) and constant separation traverse (2-D) techniques. The objectives are to (i) map the vertical and lateral extent of the regolith cover; (ii) delineate regolith constituents, layer thicknesses and electrical characteristics (resistivity and anisotropy coefficient); (iii) compare the geologic conditions at the stable and bad portions of the road for better understanding of the geological condition responsible for the perennial problems of pavement dilapidation.

2. Location and geology of the study area

Nasarawa State is situated in the northcentral geopolitical region of Nigeria. It lies between latitude 7° 45′ and 9° 25′ N and longitude 7° 15′ and 9° 37′ E (Figure 3). It is bounded in the north by Kaduna State, in the east by Plateau State, in the south by Taraba and Benue States and in the West by Kogi State and the Federal Capital Territory, Abuja (Figure 3). The physical features of the state are partly mountainous, some of which are rocky (Nasarawa, Nasarawa Eggon, Wamba, Keffi and Akwanga) and of undulating highlands with average height of about 1,400 m above sea level. Places such as Lafia, Doma, Awe and Keana are mainly plain terrains (Anudu et al.

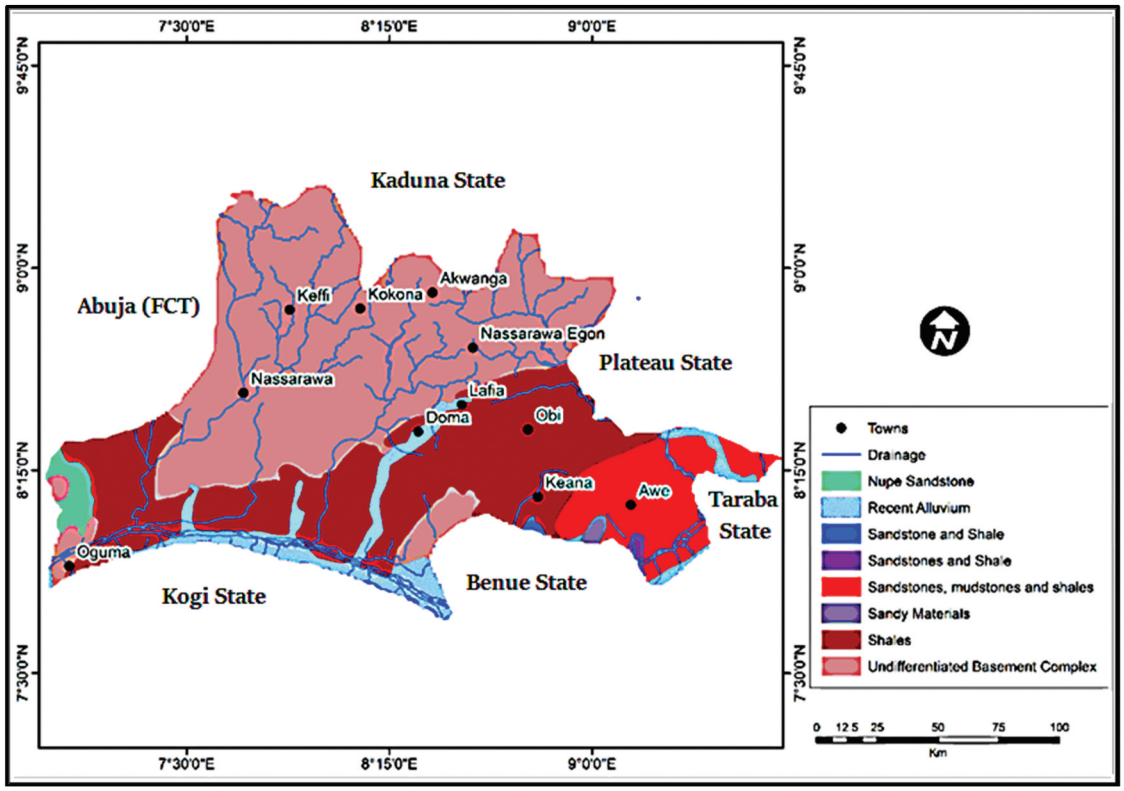

Figure 3. Generalised geological map of Nasarawa State.

2012). Soils at the foot of the hilly locations are mostly volcanic in nature and therefore loamy and rich, with the higher grounds characterised by thin soil. The area is composed of very fertile alluvial soil which has been deposited by the seasonal flood occasioned by the River Benue. The regional soils are those of sandstones derived from old sedimentary rocks with widespread occurrences of lateritic crust (Akande et al. 1988, 1989; Tukur et al. 2015).

The vegetation of Nasarawa State is of the Savannah type (Ideki and Weli 2019; Oladeinde et al. 2020). The annual rainfall varies between 111.7 mm and 145.0 mm, and the relative humidity ranges around 60–80%, with annual temperature varying from a minimum of 17℃ for a very cold day to a maximum of 35℃ for a very hot day. The average annual sunshine hour is about 6.7 per day (Oladeinde et al. 2020). The cold months due to the Harmattan wind blowing from the Northeast are December, January and February. It has two characteristic and distinct seasons: dry (November to February) and rainy (March to October). This state has rich deposits of several solid minerals of economic values such as gemstones, barites, gypsum, kaolin and marble which are yet to be exploited (Adewumi and Salako 2018).

Nasarawa State is partly underlain by Basement Complex rocks (60%) and partly by sedimentary rocks (40%) of the Benue Trough (Chaanda et al. 2010; Adewumi and Salako 2018). The elevated Precambrian Basement Complex regions are composed of older granite, gneiss and migmatite. While the deep zones are filled with Cretaceous sediments accumulated subsequent to the Mesozoic evolution of the Benue Trough's subsided graben structure (Wright 1981; Obaje 2009; Chaanda et al. 2010). The Benue trough has been geographically divided into three parts: lower, middle and upper divisions (Offodile 1980). Nasarawa State falls within the middle Benue Trough, which is a Cretaceous–Tertiary sediment which predates the mid-Santonian (Benkhelil 1989; Obaje 2009; Ogundipe 2017). Its southern limit has a boundary with the northern segment of the Niger Delta Basin, while its northern limit shares a boundary with the southern segment of the Chad Basin (Obaje 2009). The middle Benue Trough is an intracratonic Cretaceous rift basin which covers the areas than span from Makurdi through Yandev, Lafia, Obi, Jangwa to Wukari (Anudu et al., 2019). Along the Obi/Lafia area, the stratigraphic succession consists of six Upper Cretaceous formations (Figure 4), made up of the Asu River Group which include the Albian Arufu, Uomba and Gboko Formations (Offodile 1976; Nwajide 1990). The lithologic column of the Asu River Group is about 1,800 m thick and consists of limestones, shales, micaceous siltstones, mudstones and clays (Offodile 1976; Offodile and Reyment 1976; Chaanda et al. 2010). The Cenomanian–

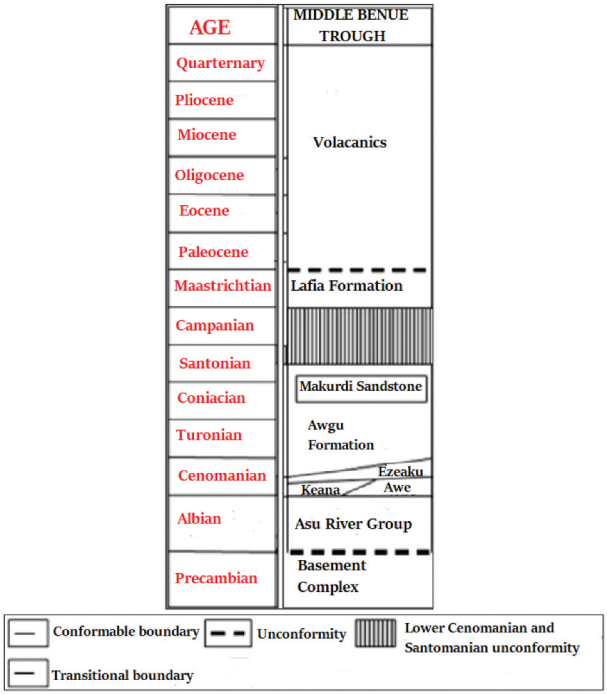

Figure 4. The stratigraphy of the Middle Benue Trough (modified from Abubakar 2014).

Turonian Keana, Awe and Ezeaku Formations overlie the Asu River Group (Offodile 1980; Wright et al. 1985). The Awe Formation deposited as transitional beds in the Late Albian Early Cenomanian regression appeared near Awe, with a thickness of about 100 m (Offodile 1976). This formation comprises flaggy, whitish, medium to coarse grained calcareous sandstones, carbonaceous shales and clays. The Keana Formation came into existence through the Cenomanian regression and deposition of fluvio-deltaic sediments. It is made up of cross-bedded, coarse-grained feldsparthic sandstones, discontinuous conglomerates and bands of shales and limestones towards the top. The origin of the Ezeaku Formation is ascribed to the commencement of marine transgression in the Late Cenomanian (Figure 4). Its major sediments are calcareous shales, micaceous fine to medium friable sandstones and beds of limestones. The deposition occurred in a supposedly shallow marine coastal environment. The deposition of the Awgu Formation terminates the process of marine sedimentation in the Benue Trough. Its main constituents are bluish-grey to dark-black carbonaceous shales, calcareous shales, shaley limestones, limestones, sandstones, siltstones and coal seams. The existence of some variety of arenaceous foraminifera in the Awgu Formation provides evidence that the deposition occurred in marshy, deltaic and shallow marine conditions (Obaje 2009; Chaanda et al. 2010). The Lafia Formation as the youngest formation was deposited under continental condition (fluviatile) in the Maastrichtian and overlies the Awgu Formation

(Figure 4). Its lithology is characterised by ferruginized sandstones, red, loose sands, flaggy mudstones, clays and claystones (Benkhelil 1989; Adewumi and Salako 2018).

3. Materials and method

3.1. Data acquisition and processing

With the goal of delineating and deciphering the subsurface conditions along Lafia-Shendam Road, the traverses outlined for the field data acquisition exercise covered both stable and collapsed sections of the road. Traverses 2 (VES 11–20) and 4 (VES 31–40) were positioned parallel and opposite to traverses 1 (VES 1–10) and 3 (VES 21–30), respectively (Figure 5). Both 1-D and 2-D electrical resistivity techniques were employed for greater confidence in interpretation. The 2-D profile was used to mitigate the limitations of the 1-D models and to give a more accurate representation of vertical and lateral resistivity distributions. The inability of the 1-D sounding techniques to incorporate lateral variations in layer resistivity is its major demerit (Loke and Barker, 1996). The basic field equipment for this study included the Ohmega resistivity meter (displays resistance values digitally) with its accessories, and global positioning system (GPS) to record the geographic coordinates and elevation of each sounding point. Schlumberger electrode array was employed for VES data acquisition at all the 40 stations, with current electrode spacing (AB/2) varied between 1 and 100 m. The potential electrode spacing (MN/2) was also varied from 0.25 to 5 m. For the CST data acquisition, a total spread of 200 m was covered along each of the four traverses with probing depth of about 50 m. For each electrode movement the resistance (R), for both VES and CST procedures were measured and the geometric factor (K) calculated based on the electrode arrangement. The apparent resistivity (ρ_a) values were computed using the product of the values of K and R. The computed apparent resistivity values were interpreted quantitatively through partial curve matching technique by plotting apparent resistivity values against the half current electrode spacings (AB/2) on a log–log graph, to generate the layer resistivities and thicknesses (Orellana and Mooney, 1966). The obtained results were fed into a computer iteration software WinResist version 1.0 (Vander-Velpen 1988), to smoothen the data points and generate the iterated values of layer resistivities and thicknesses. Surfer 12 software was used for the processing of the CST data. The interpreted VES and CST data were used to generate the geoelectric sections and 2D resistivity structures, respectively.

4. Computation of second-order geoelectric parameters

Anisotropy of weathered medium (regolith) is considered because the process of weathering of hard rock is not a uniform phenomenon and often results in heterogeneous

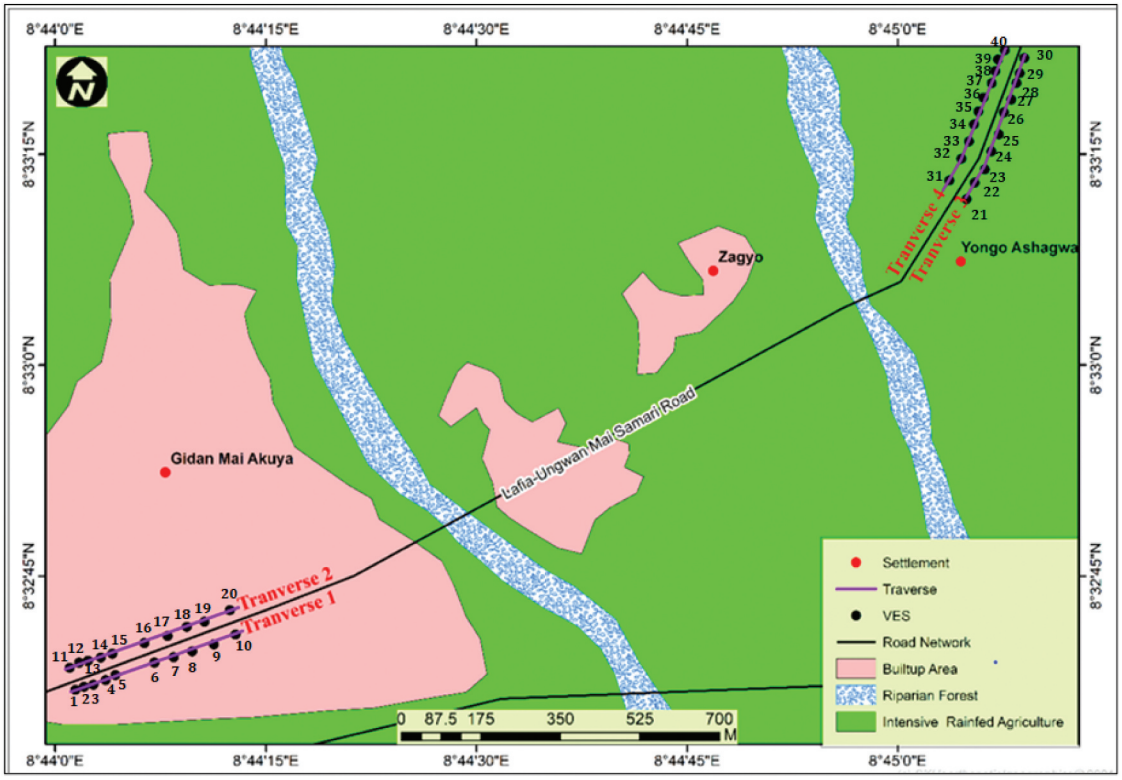

Figure 5. Base map of the study area showing the layout of the traverses and VES stations.

geologic as well as hydrological characteristics of the rock formations (Finkl 1988; Anand, 2016). In layered rocks, the Dar Zarrouk or second-order geoelectric parameters (longitudinal resistivity ρ_L and transverse resistivity ρ_T) are useful for the treatment of a sequence of layered dissimilar isotropic materials behaving as a single (bulk), equivalent anisotropic unit (Maillet 1947; Zohdy et al. 1974; Henriet 1976; Christensen 2000). The assumption here is that the conductivity is uniform in all horizontal directions but varies in the vertical direction (transversely isotropic layered model). Hence, the resistivity parallel to the layering (ρ_L) is always less than the perpendicular to the layering (ρ_T). Two other quantities, the average resistivity, ρ_m and the resistivity anisotropy coefficient, λ useful for determining the pseudo-anisotropy of layered geologic sequence are given as:

$$\lambda = \sqrt{\frac{\rho_T}{\rho_L}} \tag{1}$$

$$\rho_m = \sqrt{\rho_T \rho_L} \tag{2}$$

$\rho_L = \sum h_i / \sum S_i$ where $S_i = h_i/\rho_i$
$\rho_T = \sum T_i / \sum h_i$ where $T_i = \rho_i h_i$
S_i and T_i are the longitudinal unit conductance and transverse unit resistance, respectively.

First-order geoelectric parameters (layer resistivities and thicknesses) from VES analysis were used to compute second-order geoelectric parameters for the regolith materials at each sounding stations. This aims to give some valuable information about the main subsurface components of the regolith of the study area, such as fine-grained clayey bodies (laterite), alluvial sand deposits or saprolite (gravel/pebbles).

5. Results

The results of this study are presented as geoelectric pseudo-sections, 2-D resistivity images and a table of Dar Zarrouk parameters. The resistivity sounding curve types obtained from the VES interpretation include simple three-layer, H, four-layer QH and more complex five-layer QQH models. These curve types all indicate the existence of a highly resistive last layer as the zone where current flow is terminated in a typical Basement Complex terrain. QH curve type is predominant, accounting for 87.5%, while H and QQH types constitute 7.5% and 5%, respectively. Samples of these curves are presented in Figure 6. Figures 7–10 show the geoelectric sections generated from VES interpretation placed above the 2-D resistivity structures from CST data processing using Surfer 12 software. The two representations in terms of the variation of resistivity distribution essentially reveal three to five geologic layers which include

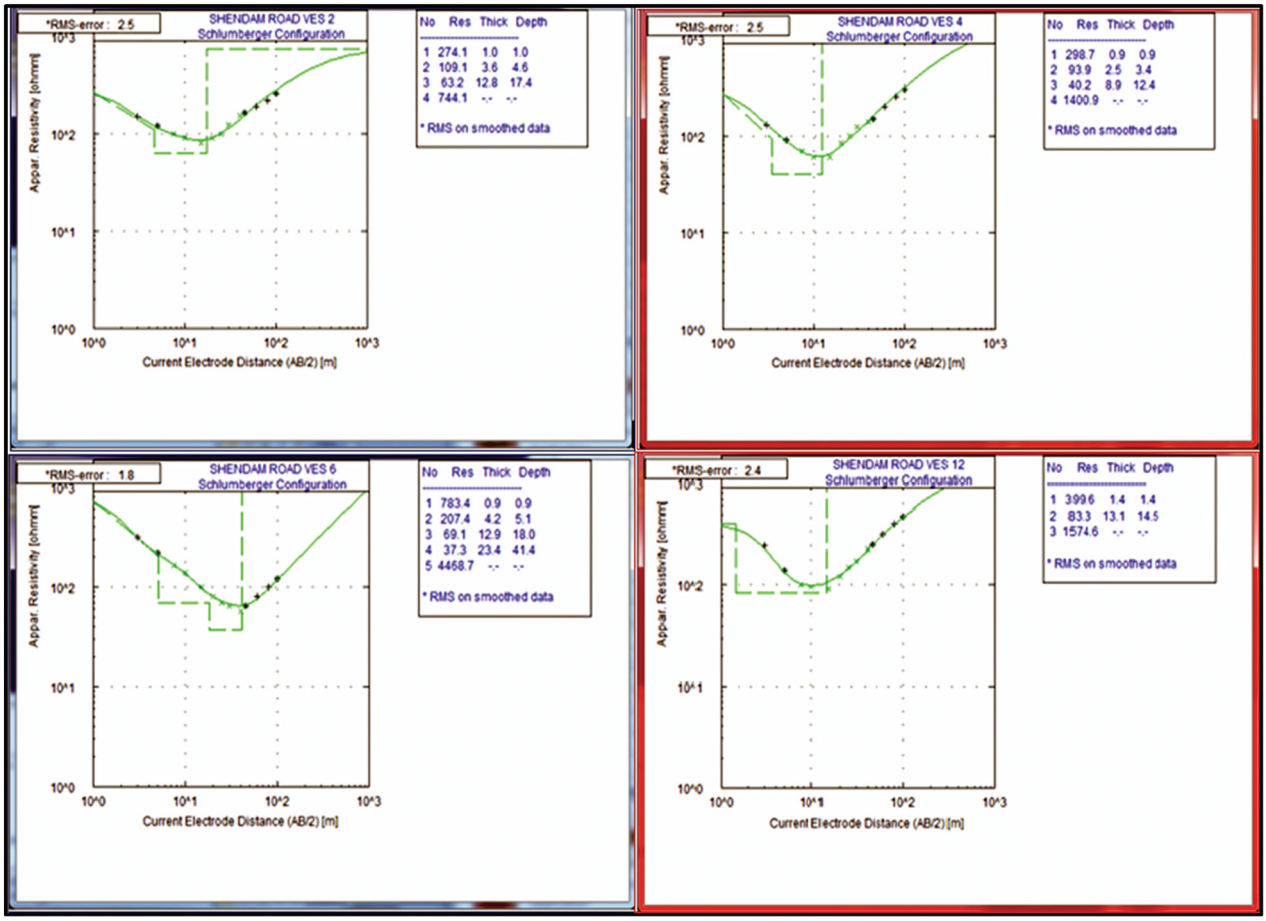

Figure 6. Samples of VES obtained after computer iteration using WinResist software.

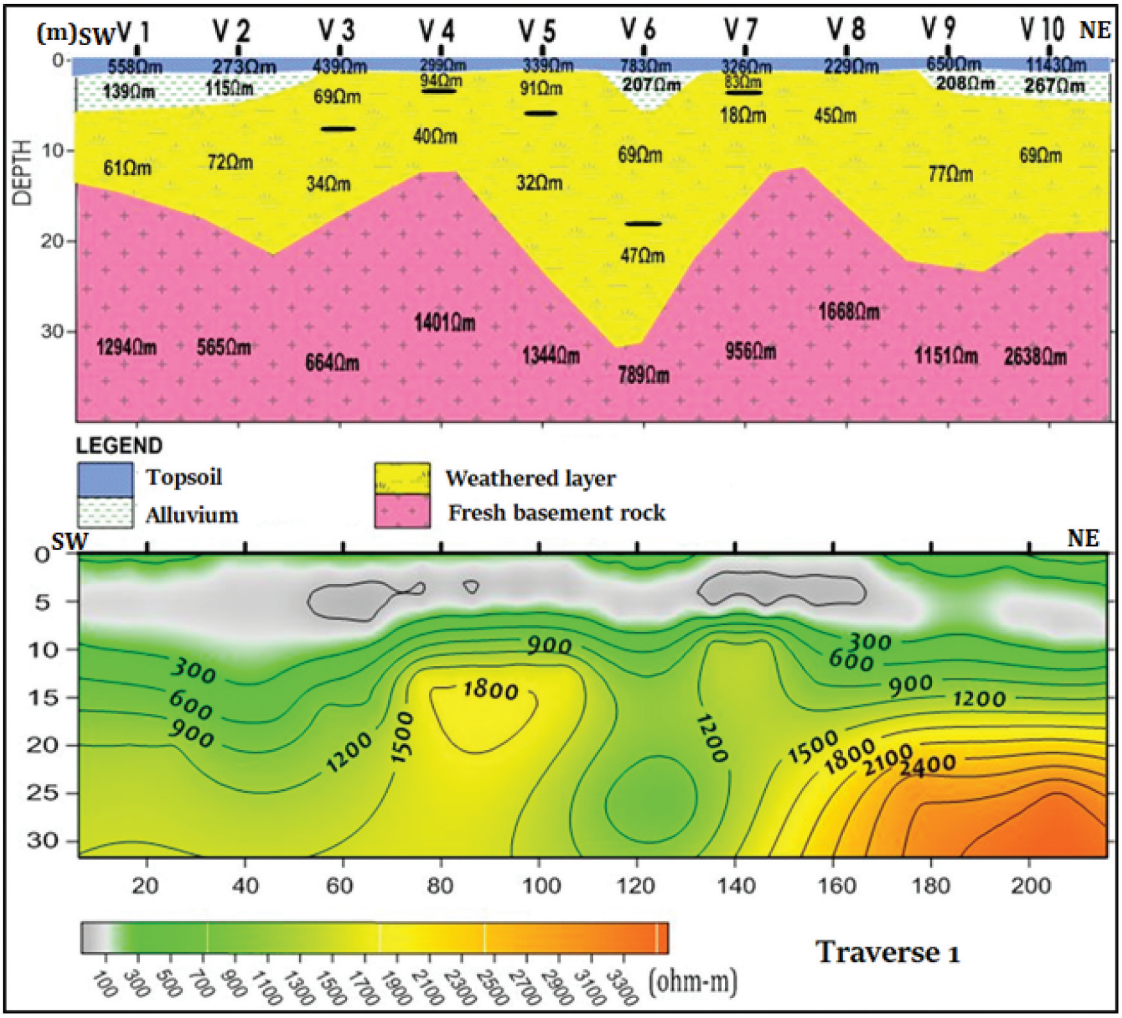

Figure 7. Geoelectric pseudo-section (VES 1–10) and 2-D resistivity image for traverse 1.

moderate/high resistive topsoil, moderate resistivity alluvium (at some locations), low resistivity clay-like or lateritic layer, very thin saprolite zone (delineated at a depth of about 10 m directly above the fresh bedrock only through CST technique) and high resistivity fresh basement rocks. The second-order geoelectric parameters computed from the results of VES interpretation are presented in Table 1.

6. Discussion

6.1. Subsurface layers' resistivities and thicknesses

VES results show generally a resistivity distribution that has a maximum of five and a minimum of three geoelectric layers, viz. first layer (topsoil), second layer (moderate resistivity alluvium deposit or laterite), third layer (laterite), fourth layer (saprolite) and fifth layer (fresh basement rocks). Both VES and CST electrical resistivity techniques reveal similar subsurface geological representations. Saprolite occurrence in the weathered zone is not clearly differentiated from the laterite layer in the geoelectric pseudo-sections generated based on the VES results. However, the saprolite medium is revealed as a very thin medium of moderate resistivity values in the 2-D resistivity images.

6.2. Traverse 1 (VES 1–10)

On the 1-D geoelectric sections (Figure 7), traverse 1 which depicts regolith thickness in the range 9.4–44.8 m is mainly a four geoelectric layer structure except at sounding stations 6 and 8 with five and three geoelectric layer structures, respectively. The first layer is the topsoil. It has resistivity and thickness values ranging from 229 to 1143 Ωm and 0.7 to 1.1 m, respectively. The resistivity range indicates the inhomogeneous composition of the topsoil materials. The second layer at sounding stations 1, 2, 6, 9 and 10 is depicted as a moderate resistivity layer in range 115–267 Ωm (Figure 7). This layer is presumably composed of alluvium sand deposits which is most likely responsible for the stable pavement at the top. Its thickness and depth ranges are 2.6–4.9 m and 3.0–5.8 m, respectively. The weathered layer is probably a mix of laterite and saprolite with resistivity range 18–77 Ωm, which constitutes the second layer at sounding stations 3, 4, 5, 7 and 8 which

Table 1. Summary of computed Dar Zarrouk parameters from VES analysis.

VES No.	Longitudinal Conductance S	Transverse Resistance T	Longitudinal Resistivity ρ_L	Transverse Resistivity ρ_T	Anisotropy λ	Mean resistivity ρ_m
1	0.2829	2043.12	73.17	98.70	1.16	84.98
2	0.2383	1648.22	78.90	87.67	1.05	83.17
3	0.4638	1354.79	44.64	65.45	1.21	54.05
4	0.2510	861.36	49.00	70.03	1.20	58.58
5	0.6883	1352.70	37.48	52.43	1.18	44.33
6	0.9166	3524.03	48.88	78.66	1.27	62.01
7	0.3718	559.04	25.28	59.47	1.53	38.78
8	0.3314	904.63	47.37	57.62	1.10	52.25
9	0.3542	2940.96	82.45	100.72	1.11	91.13
10	0.2799	3366.44	81.10	148.30	1.35	109.67
11	0.2708	820.45	41.36	73.25	1.33	55.04
12	0.1608	1650.67	90.19	113.84	1.12	101.33
13	0.1573	912.70	60.38	96.07	1.26	76.16
14	0.4567	3193.36	73.58	95.04	1.14	83.62
15	0.3202	851.30	44.35	59.95	1.16	51.57
16	0.2706	941.79	46.93	74.16	1.26	58.99
17	0.2083	2481.73	70.08	169.98	1.56	109.15
18	0.3504	1087.73	37.38	83.03	1.49	55.71
19	0.2955	2180.48	62.60	117.86	1.37	85.89
20	0.2333	2845.24	80.58	151.34	1.37	110.43
21	0.4077	4440.06	92.96	117.15	1.12	104.36
22	0.3381	3702.86	83.71	130.84	1.25	104.65
23	0.2948	812.83	36.64	75.26	1.43	52.51
24	0.4003	3152.64	59.21	133.02	1.50	88.75
25	0.1944	1831.91	61.22	153.94	1.59	97.08
26	0.3815	922.59	34.87	69.37	1.41	49.18
27	0.4194	4012.92	70.34	136.03	1.39	97.82
28	0.1896	2684.83	92.85	152.55	1.28	119.01
29	0.2943	1020.53	46.21	75.04	1.27	58.88
30	0.4345	2496.83	60.53	94.94	1.25	75.81
31	0.3535	950.89	45.83	58.70	1.13	51.86
32	0.5166	3460.56	63.30	105.83	1.29	81.85
33	0.2761	2841.02	83.32	123.52	1.22	101.45
34	0.1756	2254.47	76.87	167.00	1.47	113.30
35	0.4579	2055.59	61.37	73.15	1.09	67.01
36	0.3126	1124.16	47.02	76.47	1.28	59.97
37	0.2563	871.22	42.92	79.20	1.36	58.30
38	0.2754	970.85	52.65	66.96	1.13	59.37
39	0.2499	2764.62	87.23	126.82	1.21	105.17
40	0.2003	1820.53	71.90	126.43	1.33	95.34

corresponds to the failed segments of the road. The thickness of the third layer ranges from 6.0 to 26.2 m at depths of 9.4 to 41.4 m. VES 5 consists of two weathered layers which is evident from its five-layer configuration. The last horizon is a highly resistive fresh basement with resistivity values ranging from 565 to 2638 Ωm. The 2-D resistivity image shown in Figure 7 reveals mainly four subsurface zones, viz. moderate resistivity (green medium at the top, 290–600 Ωm) which corresponds to the alluvium deposit at some locations, low resistivity laterite (<120 Ωm) in the upper two layers at some locations, deeper moderate resistivity (about 300 Ωm) thin saprolite layer directly above the high resistivity (900–2400 resistivity) fresh basement rock.

6.3. Traverse 2 (VES 11–20)

This traverse is nearly opposite and parallel to traverse 1. Regolith thickness across the traverse as shown in Figure 8 is in the ranges from 9.5 to 33.6 m. VES interpretation for stations 12 and 13 shows a three geoelectric layer structure, while the remaining eight stations (11, 14–20) are four-layer structures. Non-uniform topsoil resistivity and thickness vary from 240 to 724 Ωm and 0.9–1.7 m, respectively. The second layer beneath stations 14, 17, 19 and 20 which show stable pavement disposition (Figure 8), consist of alluvium deposit, which has moderate resistivity and thickness values ranging from 145 to 250 Ωm and from 3.7 to 6.1 m, respectively. However, the second and third layers beneath VES stations 11–13, 15, 16 and 18 are a weathered horizon which has resistivity values from 21 to 83 Ωm and thickness from 5.7 to 27.6 m. The last medium is the highly resistive fresh basement of resistivity ranging from 554 to 2773 Ωm. Four subsurface zones are clearly shown on the 2-D resistivity pseudosection (Figure 8), similar to traverse 1. The layer sequence encompasses an uppermost moderate resistivity (180–550 Ωm) alluvium deposit, low resistivity laterite (<120 Ωm), thin and deeper zone of moderate resistivity (190–380 Ωm) saprolite layer directly above the high resistivity (590–2190 Ωm) fresh basement rock.

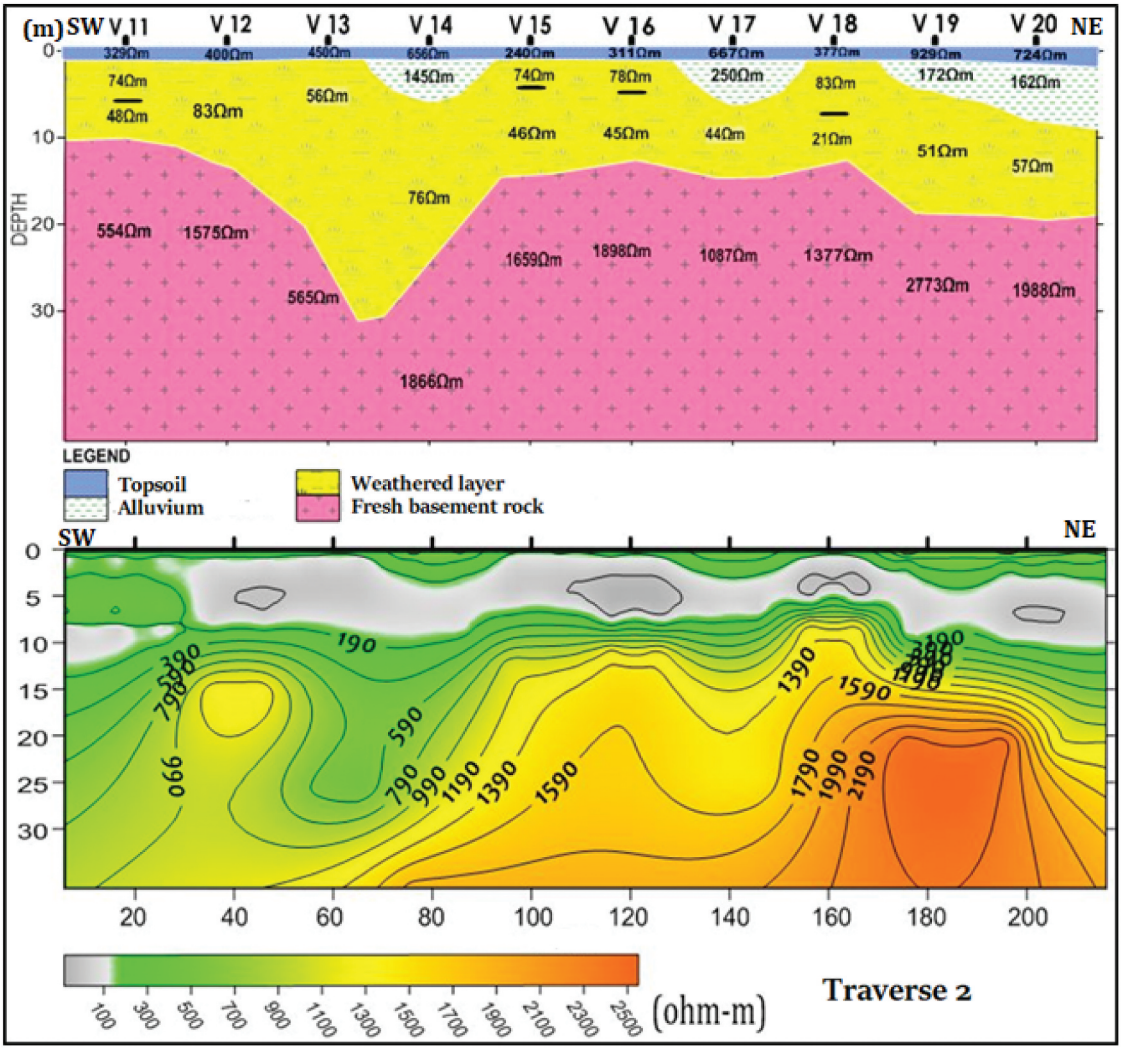

Figure 8. Geoelectric pseudo-section (VES 11–20) and 2-D resistivity image for traverse 2.

6.4. Traverse 3 (VES 21–30)

1-D interpretation of traverse three (Figure 9) depicts regolith thickness ranges from 10.8 to 38.0 m. It is dominated by a four-layer resistivity structure at nine sounding stations (22–30). The exception is VES 21 which is a three-layer geoelectric structure in which the second and third strata combine to give the weathered layer. The resistivity and thickness of the heterogeneous topsoil on this traverse range from 367 to 1163 Ωm and 0.7 to 1.2 m, respectively. The stable road segments at the top of stations 21, 22, 24, 25, 27, 28 and 30 (Figure 9) are underlain by a second layer that is likely an alluvium deposit at a depth ranging from 4.1 to 6.0 m. The resistivity and thickness values of this layer are in the range 141–284 Ωm and 3.3–5.0 m, respectively. The second layer beneath other sounding stations (23, 26 and 29) as well as the third layer along this traverse are composed of laterite with resistivity and thickness ranges obtained as 25–97 Ωm and 6.1–24.4 m, respectively. The last medium is the fresh basement rock which has resistivity ranging from 717 to 3489 Ωm. The 2-D resistivity imaging pseudosection (Figure 9) reveals mainly four subsurface zones, viz. moderate resistivity (green section at the top), which is alluvium deposit with resistivity distribution of 180–600 Ωm, low resistivity laterite having resistivity less than 120 Ωm, deeper and thin layer of saprolite having moderate resistivity of about 380 Ωm overlying the highly resistive (780–2780 Ωm) fresh basement rock.

6.5. Traverse 4 (VES 31–40)

Interpretated results suggest a four-layer model for the area covered by the 10 VES points. The estimated regolith thickness ranges from 11.0 to 32.8 m. The inhomogeneous topsoil has resistivity and thickness values lying in the range 250–1061 Ωm and 0.8–1.3 m, respectively. Similar to traverse three, pavement above sounding stations 32, 33, 34, 39 and 40 appeared stable (Figure 10). The second layer (alluvium deposit) underlying these stations is at depth range of 3.6–5.2 m, has moderate resistivity that ranges from 198 to 240 Ωm with thickness range of 2.5–4.2 m. The weathered layer composed of laterite and saprolite encountered at a depth range of 11.0–32.8 m has low

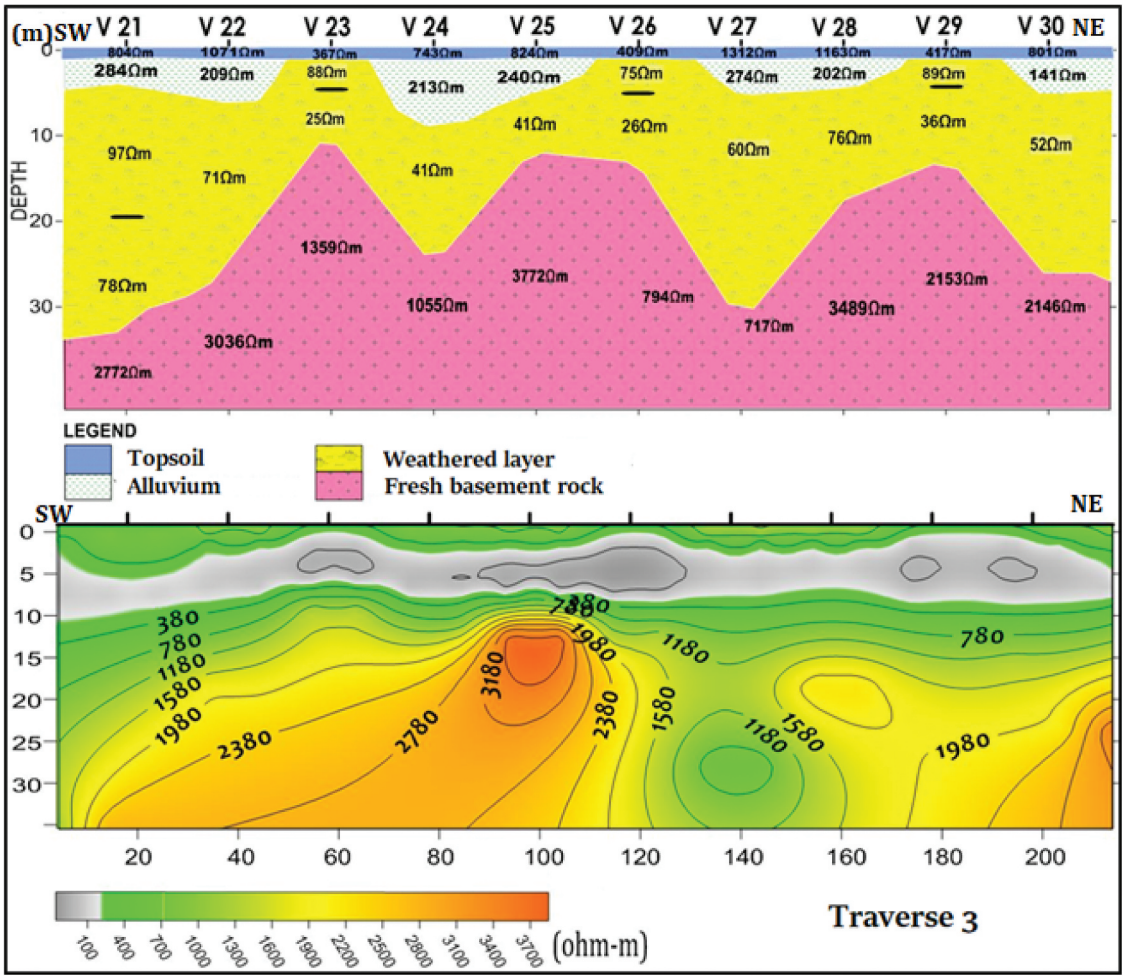

Figure 9. Geoelectric pseudo-section (VES 21–30) and 2-D resistivity image for traverse 3.

resistivity values of 32–93 Ωm with thickness 7.0–27.6 m. Current terminates at the resistive fresh basement with resistivity range 542–3142 Ωm. The 2-D resistivity imaging pseudosection reveals primarily a four-layer subsurface zones, viz. moderate resistivity (green medium at the top, 200–600 Ωm) alluvium deposit, low resistivity laterite (<120 Ωm), deeper moderate resistivity (310 Ωm) thin saprolite layer directly above the high resistivity (970–1960 Ωm) fresh basement rock.

In geotechnical consideration, a good subgrade material should be able to support the loads transmitted from the pavement structure. This load bearing capacity of a subgrade material is usually affected by the degree of compaction, moisture content and soil type. A subgrade that can support a large load without excessive deformation is considered good. Across the study area, the average thickness of the delineated regolith, which is majorly lateritic, ranges from 10.2 to 37.3 m. Laterite belongs to the clay family. These expansible (shrink-swell), very unstable and easily deformable (i.e. plastic) soils pose widespread geological hazards globally. They present significant geotechnical and structural challenges to buildings and roads. The characteristic volume change is a result of changes in their moisture content. Swelling pressures can cause heave, or lifting of structures, whilst shrinkage can cause settlement or subsidence, which may be differential. Hence, road pavement laid directly above this expansible soil are prone to degradation and dilapidation. Conversely, sand has large particles which allow this soil to drain water quickly, which is good for stability of structures and roads. The retention of less water implies lower risk for the building to shift around and form structural and non-structural cracks. The failed segments of the road were underlain by lateritic second and third subsurface layers directly above the saprolite zones and the fresh basement rock. While at the stable segments, the second geoelectric layer is composed of alluvium sand deposit of moderate thickness above laterite medium.

7. Resistivity coefficient of anisotropy and regolith characteristics

Due to the recognition of the importance of homogeneity and anisotropy concepts in electrical and

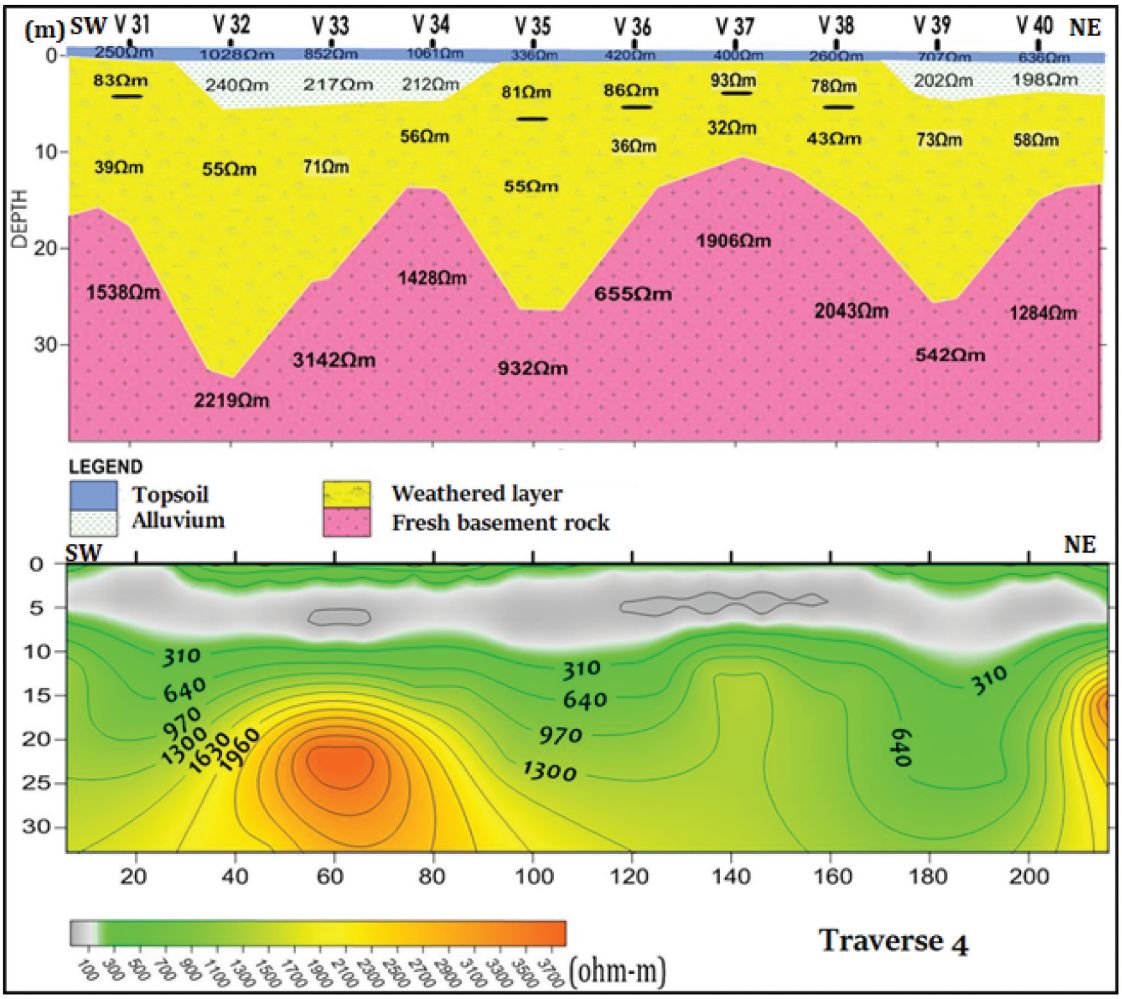

Figure 10. Geoelectric pseudo-section (VES 31–40) and 2-D resistivity image for traverse 4.

electromagnetic modelling, the evaluation of Dar Zarrouk parameters (longitudinal, transverse and mean resistivities, coefficient of anisotropy) was incorporated into the 1-D VES analysis and interpretation. This is to provide further insights on the subsurface condition so as to decipher the presence and contribution of thin layer of saprolite to the overall electrical properties of regolith in the study area. In hydrogeological investigations, the coefficient of anisotropy suggests the existence of layers that could significantly affect groundwater flow and functions as a quality indicator in the characterisation of geological raw materials (Christensen 1992). Table 1 shows explicitly that the values of longitudinal resistivity are reasonably lower than those of transverse resistivity for all the sounding stations which is in agreement with the findings of Flathe (1955). This confirms the already established theoretical fact that current flow and mean hydraulic conduction parallel to geologic boundaries (longitudinal) are greater relative to those normal to the boundary plane (transverse). These two resistivities are also the inputs for computing the average resistivity,$\rho_m$and the resistivity anisotropy coefficient, λ. Furthermore, the variations in the computed λ andρ_m for the subsurface sequence in the study area indicate that the degree of heterogeneity (different constituents) of the regolith cover is considerably low (Christensen 1992). This suggests that the regolith is more composed of clayey substances (laterite) than saprolite, which is composed of fragmented rock pieces in the form of pebbles and gravel. More intense weathering leads to the continuous transition from saprolite to laterite. In addition, saprolite is more often form in the lower zones of soil horizon arising from deep disintegration or weathering of bedrock surface. The ranges for λ are as follows: 1.05–1.53 (traverse one); 1.12–1.56 (traverse two); 1.12–1.59 (traverse three); and 1.09–1.47 (traverse four). Anisotropy is usually most pronounced in fine-grained lithologies, such as silt, clay, etc., and less well developed in coarse-grained lithologies like sand, gravel, etc. (Merritt et al., 2016). Therefore, the gravel-like saprolite constituents in the regolith could be responsible for the low values of $\lambda.\rho_m$ ranges across the traverses are as follows: 38.18–109.67 Ωm (traverse 1); 51.57–110.43 Ωm (traverse 2); 49.19–119.01 Ωm (traverse 3); and 51.86–113.30 Ωm (traverse 4). These resistivity variations further point to the existence of a greater proportion of laterite than saprolite in the regolith volume at the study location. Hence, it is evident that the lithology and sedimentology of subsurface structures are of profound effect on

the directional anisotropy of electrical properties of geological materials (Merritt et al., 2015). Naturally occurring lateritic soils (silty, clay-rich materials) do not make appropriate fill material for road construction projects due to their poor bearing capacity. Therefore, laying pavement directly on lateritic soil should be avoided in road construction projects. However, adding a stabilising agent like cement or lime may alter the properties of this geotechnically weak soil. Consequently, additives are frequently used to enhance the performance of laterite soil-based pavements.

8. Conclusion

In this study, the electrical characteristics and structures of the regolith cover along Lafia-Shendam Road have been investigated using electrical resistivity techniques. The regolith thickness varies from very low to moderately high values with average values lying within the range 10.2–37.3 m. Combined interpretation from geoelectric sections and 2-D imagings reveal a maximum of five (5) and a minimum of three (3) geoelectric layers, viz. the first geoelectric layer corresponds to the topsoil which has resistivity and thickness values ranging from 229 to 1163 Ωm and 0.7 to 1.7 m, respectively. The second layer consists of alluvium deposit and has resistivity and thickness values ranging from 115 to 284 Ωm and 2.6 to 6.1 m, respectively. The third layer is composed of a weathered layer deposit with resistivity and thickness values ranging from 18 to 97 Ωm and 5.7 to 27.6 m, respectively. The fourth subsurface zone is the highly resistive fresh bedrock. Its resistivity values vary from 542 to 3489 Ωm.

Saprolite occurrence in the weathered layer, which is masked in the VES interpretation, is delineated as a thin zone of moderate resistivity values in the 2-D resistivity images. Dar Zarrouk parameters (longitudinal and transverse resistivities, coefficient of anisotropy) obtained from the VES results show that the values of longitudinal resistivity are generally lower than those of transverse resistivity for all the VES points. On average, the coefficient of anisotropy λ and mean resistivity ρ_m vary in the ranges 1.10–1.54 and 47.70–113.10 Ωm, respectively, which implies that the degree of heterogeneity of the constituents of the regolith is considerably low. The gravel-like saprolite constituents in the regolith account for the low values of λ. The lower limit of $\rho_m$values is above the typical values expected for clay-rich materials, while the upper limits are significantly less than the characteristic resistivity values for fractured bedrock. These resistivity values reveal a greater proportion of laterite than saprolite in the regolith volume at the study location. This aspect is now included. Due to their weak bearing ability, naturally occurring lateritic soils (silty, clay-rich materials) when untreated, are not suitable as good fill material for road construction projects. However, stabilisation of this geotechnically poor soil with additive substance such as cement or lime, etc., might improve their geotechnical characteristics. Hence, in order to improve the performance of laterite soil-based pavements, additives are typically utilised.

Acknowledgments

The authors wish to appreciate Mr G.S. Chunmada and his technical team for the assistance rendered in the data acquisition exercise. Mr T. Adeleke is also appreciated for his technical contribution towards the completion of the study.

Disclosure statement

No potential conflict of interest was reported by the author(s).

Funding

No funding was received to accomplish this study.

ORCID

Olawale Babatunde Olatinsu http://orcid.org/0000-0002-0412-1972

Availability of data and material

The data used for this study are confidential.

Consent for publication

The two authors mutually agreed and gave their consent for this article to be published.

Ethics approval and consent to participate

This article does not contain any studies involving life, whether animal or human, performed by any of the authors.

References

Abubakar MB. 2014. Petroleum potentials of the Nigerian Benue Trough and Anambra Basin: a regional synthesis. Nat Resour. 5(1):25–58. doi: 10.4236/nr.2014.51005.

Acworth RI. 1987. The development of crystalline basement aquifers in a tropical environment. Q J Eng Geol Hydrogeol. 20(4):265–272. doi: 10.1144/GSL.QJEG.1987.020.04.02.

Adebisi NO, Ariyo SO, Sotikare PB. 2016. Electrical resistivity and geotechnical assessment of subgrade soils in southwestern part of Nigeria. J Afr Earth Sci. 119:256–263. doi: 10.1016/j.jafrearsci.2016.03.019.

Adewumi T, Salako KA. 2018. Delineation of mineral potential zone using high resolution aeromagnetic data over

part of Nasarawa State, North Central Nigeria. Egypt J Pet. 27(4):759–767. doi: 10.1016/j.ejpe.2017.11.002.
Agbede OA. 1992. Characteristics of tropical red soils as foundation materials. Nigerian J Sci. 26:237–242.
Akande SO, Horn EE, Reutel C. 1988. Mineralogy, fluid inclusion and genesis of the Arufu and Akwana Pb-Zn-F mineralization, middle Benue Trough, Nigeria. J Afr Earth Sci. 7:167–180. doi: 10.1016/0899-5362(88)90063-2.
Akande O, Zentelli M, Reynolds PH. 1989. Fluid inclusion and stable isotope studies of Pb-Zn-fluorite-barite mineralization in the lower and middle Benue Trough, Nigeria. Mineral Deposita. 24(3):183–191. doi: 10.1007/BF00206441.
Anand RR. 2016. Regolith-landform processes and geochemical exploration for base metal deposits in regolith-dominated terrains of the Mt Isa region, northwest Queensland, Australia. Ore Geol Rev. 73:451–474. doi: 10.1016/j.oregeorev.2015.08.014.
Anand RR, Butt CRM. 1988. The terminology and classification of the deeply weathered regolith. Perth, Western Australia: CSIRO, Division of Exploration Geoscience.
Anudu1 GK, Onuba LN, Onwuemesi AG, Ikpokonte AE. 2012. Analysis of aeromagnetic data over Wamba and its adjoining areas in north-central Nigeria. Earth Sci Res J. 16(1):25–33. doi: 10.3923/rjasci.2012.1.9.
Anudu GK, Stephenson RA, Ofoegbu CO, Obrike SE. 2019. Basement morphology of the middle Benue Trough, Nigeria, revealed from analysis of high-resolution aeromagnetic data using grid-based operator methods. J Afr Earth Sci. 162:103724. doi: 10.1016/j.jafrearsci.2019.103724.
Benkhelil J. 1989. The origin and evolution of the Cretaceous Benue Trough (Nigeria). J African Earth Sci. 8(2–4):251–282. doi: 10.1016/s0899-5362(89)80028-4.
Biggs AJW, Mahony KM. 2004. Is soil science relevant to road infrastructure? 13th International Soil Conservation Organisation Conference; July; Brisbane, Australia.
Bishop J, Sattel D, Macnae J, Munday T. 2001. Electrical structure of the regolith in the Lawlers District, Western Australia. Explor Geophys. 32(1):20–28. doi: 10.1071/eg01020.
Butt CRM, Lintern MJ, Anand RR. 1997. Evolution of regoliths and landscapes in deeply weathered terrain – implications for geochemical exploration. Ore Geol Rev. 16(3–4):167–183. doi: 10.1016/S0169-1368(99)00029-3.
Camarero PL, Moreira CA. 2017. Geophysical investigation of earth dam using the electrical tomography resistivity technique. Rem Revista Escola de Minas. 70(1):47–52. doi: 10.1590/0370-44672016700099.
Chaanda MS, Obaje NG, Moumouni A, Goki NG, Lar UA. 2010. Environmental Impact of artisanal Mining of Barytes in Azara Area, Middle Benue Trough, Nigeria. Online J Earth Sci. 4(1):38–32. doi: 10.3923/ojesci.2010.38.42.
Chardon D, Grimaud J, Beauvais A, Bamba O. 2018. West African lateritic pediments: landform-regolith evolution processes and mineral exploration pitfalls. Earth Sci Rev. 179:124–146. doi: 10.1016/j.earscirev.2018.02.009.
Christensen NB. 1992. On the importance of determining electrical anisotropy in hydrogeological investigations. 54th EAEG meeting, Paris, France, Extended Abstracts. p. 712–713.
Christensen NB. 2000. Difficulties in determining electrical anisotropy in subsurface investigation. Geophys Prospect. 48(1):1–19. doi: 10.1046/j.13652478.2000.00174.x.
Chunwate BT, Yahaya S, Samaila IK, Ja'afaru SW. 2019. Analysis of urban land use and land cover change for sustainable development: a case of Lafia, Nasarawa State, Nigeria. J Geogr Inf Syst. 11(3):347–358. doi: 10.4236/jgis.2019.113021.
Daud NNN, Jalil FNA, Celik S, Albayrak ZNK. 2019. The important aspects of subgrade stabilization for road construction. IOP Conf Ser: Mater Sci Eng. 512:012005. doi: 10.1088/1757-899X/512/1/012005.
Eggleton RA, Taylor G, Le Gleuher M, Foster LD, Tilley DB, Morgan CM. 2008. Regolith profile, mineralogy and geochemistry of the weipa bauxite, northern Australia. Aust J Earth Sci. 55(sup1):S17–S43. doi: 10.1080/08120090802438233.
FERMA. 2020. Report on environmental management plan (EMP) for the periodic maintenance of Lafia roads: federal roads development project (FRDP) Nigeria in collaboration with federal roads maintenance agency.
Finkl CW. 1988. Soils and weathered materials, field methods and survey. In: General geology. Encyclopedia of earth science. Boston (MA): Springer. doi:10.1007/0-387-30844-X_107.
Flathe H. 1955. Possibilities and limitations in applying geoelectrical methods to hydrogeological problems in the coastal area of northwest Germany. Interact Stud. 3(2):95–110. doi: 10.1111/j.1365-2478.1955.tb01363.x.
Georgiadis GA, Tranos MD, Makedon TK, Dimopoulos GC. 2007. Contribution of geological mapping in road construction: an example from Veria-Kozani National road, Kastania Area. Bull Geol Soc Greece. 40(4):1652–1663. doi: 10.12681/bgsg.17069.
Gourdol L, Clément R, Juilleret J, Pfister L, Hissler C. 2021. Exploring the regolith with electrical resistivity tomography in large-scale surveys: electrode spacing-related issues and possibility. *Hydrol Earth Syst Sci*. 25(4):1785–1812. doi: 10.5194/hess-25-1785-2021.
Govindan S (2015). Near surface investigations at the in-situ regolith and fresh rock interface: an investigation into the effects of a strong Fe-oxide presence on the electrical resistivity signature at Major's Creek, NSW, *SEG Global Meeting Abstracts*; 7–10 July; Near-Surface Asia Pacific Conference, Waikoloa, Hawaii. doi: 10.1190/nsapc2015-001.
Graham RC, Rossi AM, Hubbert KR. 2010. Rock to regolith conversion: producing hospitable substrates for terrestrial ecosystems. GSA Today. 20(2):4–9. doi: 10.1130/GSAT57A.1.
Gupta RK, Abrol IP, Finkl CW. 2008. Saprolite, regolith and soil. In: Chesworth W, editor. Encyclopedia of Soil Science. Encyclopedia of earth sciences series. Dordrecht: Springer. doi: 10.1007/978-1-4020-3995-9_502.
Hazell JRT, Cratchley CR, Jones CRC. 1992. The hydrogeology of crystalline aquifers in northern Nigeria and geophysical techniques in their exploration. London: Geological Society. doi:10.1144/GSL.SP.1992.066.01.08.
Hazell JRT, Cratchley CR, Preston AM. 1988. The location of aquifers in crystalline rocks and alluvium in northern Nigeria using combined electromagnetic and resistivity techniques. Q J Eng Geol Hydrogeol. 21(2):159–175. doi: 10.1144/GSL.QJEG.1988.021.02.05.
Henriet JP. 1976. Direct applications of the Dar Zarrouk Parameters in ground water surveys. Geophys Prospect. 24(2):344–353. doi: 10.1111/j.1365-2478.1976.tb00931.x.
Hobbs PRN, Jone LD, Kirkham MP, Gunn DA, Entwisie DC. 2019. Shrinkage limit test results and

interpretation for clay soils. Q J Eng Geol Hydrogeol. 52 (2):220–229. doi: 10.1144/qjegh2018-100.
Hunt CE. 1986. Surficial deposits of the United States. New York: Van Nostrand Reinhold.
Ideki O, Weli VE. 2019. Analysis of rainfall variability using remote sensing and GIS in North Central Nigeria. Atmos Clim Sci. 9(2):191–201. doi: 10.4236/acs.2019.92013.
Jone LD. 2017. Expansive soils. In encyclopaedia of engineering geology. Bobrowsky, P.T. and Marker, M., editors. London, UK: Meteor Springer.
Jones MJ. 1985. The weathered zone aquifers of the basement complex areas of Africa. Q J Eng Geol Hydrogeol. 18(1):35–46. doi: 10.1144/GSL.QJEG.1985.018.01.06.
Juilleret J, Dondeyne S, Hissler C. 2014. What about the Regolith, the saprolith and the bedrock: proposals for classifying the subsolum in WRB. European Geosciences Union General Assembly, 27 April – 02 May, 2014, Vienna, Austria.
Keller GV 1974. Engineering applications of electrical geophysical methods. In: Subsurface exploration for underground excavation and heavy construction. American Society of Civil Engineers Speciality Conference, Henniker. p. 128–143.
Keller GV, Frischknecht FC. 1996. Electrical methods in geophysical prospecting. London: Pergamon.
Kellett R, Steensma G, Bauman P. 2004. Mapping groundwater in regolith and fractured bedrock using ground and airborne geophysics: case studies from Malawi and Brazil. ASEG Ext Abstr. 2004(1):1–4. doi: 10.1071/ASEG2004ab080.
Key RM. 1992. An introduction to the crystalline basement of Africa. Geol Soc London, Spec Publ. 66:29–57. doi: 10.1144/GSL.SP.1992.066.01.02.
Loke MH, Barker RD. 1996. Rapid Least-Squares Inversion of Apparent Resistivity Pseudosections by a Quasi-Newton Method. Geophys Prospect. 44:131–152. doi: 10.1111/j.1365-2478.1996.tb00142.x.
Lowrie W, Fichtner A. 2019. Fundamentals of geophysics. 3rd ed. Cambridge, United Kingdom: Cambridge University Press.
MacDonald AM, Calow RC. 2009. Developing groundwater for secure rural water supplies in Africa. Desalination. 248(1–3):546–556. doi: 10.1016/j.desal.200-8.05.100.
MacDonald DMJ, Edmunds WM. 2014. Estimation of groundwater recharge in weathered basement aquifers, southern Zimbabwe; a geochemical approach. Appl Geochem. 42:86–100. doi: 10.1016/j.apgeochem.2014.01.003.
Maillet R. 1947. The fundamental equations of electrical prospecting. Geophysics. 12(4):529–662. doi: 10.1190/1.1437342.
Massarch KR. 2000. Geophysical methods for geotechnical, geo-environmental and geo-dynamic site characterization. In: 3rd international workshop on the applications of geophysics to rock and soil engineering, 18 November 2000, Melbourne, Australia.
Merritt AJ, Chambers JE, Wilkinson PB, West LJ, Murphy W, Gunn D, Uhlemann S. 2016. Measurement and modelling of moisture—electrical resistivity relationship of fine-grained unsaturated soils and electrical anisotropy. J Appl Geophys. 124:155–165. doi: 10.1016/j.jappgeo.2015.11.005.
Munday TJ, Macnae J, Bishop J, Sattel S. 2001. A geological interpretation of observed electrical structures in the regolith: lawlers, Western Australia. Explor Geophys. 32 (1):36–47. doi: 10.1071/eg01036.
Munday T, Sumpton J, Fitzpatrick A. 2004. Exploration for kimberlites through a complex regolith cover – a case study in the application of AEM in the deeply weathered archaean yilgarn craton, Western Australia. Paper Number: SEG-2004-1225 presented at the 2004 SEG Annual Meeting, Denver, Colorado; October.
Nwajide CS. 1990. Cretaceous sedimentation and paleogeography of the Central Benue trough. In: Ofoegbu CO, editor. The BenueTrough, Structure and Evolution. International monograph series. Braunschweig; p. 19–38.
Obaje NG. 2009. The Benue Trough. In: Geology and mineral resources of Nigeria. Lecture notes in earth sciences. Vol. 120. Berlin, Heidelberg: Springer. 10.1007/978-3-540-92685-6_5
Obiora SC. 2006. Petrology and geotectonic setting of the basement complex rocks around Ogoja, south-eastern Nigeria. Ghana J Sci. 46(1):13–25. doi: 10.4314/gjs.v46i1.15912.
Offodile ME. 1976. A review of the geology of the cretaceous of the Benue Valley. In: Kogbe CA, editor Geology of Nigeria. Lagos: Elizabethan Publishing Co. pp. 319–330.
Offodile ME. 1980. A mineral survey of the cretaceous of the Benue Valley, Nigeria. Cretaceous Res. 1(2):101–124. doi: 10.1016/0195-6671(80)90020-8.
Offodile ME, Reyment R. 1976. Stratigraphy of the Keana-Awe area of the middle Benue 435 region of Nigeria. Bull Geol Institut Univ Upsala. 7:37–66.
Ogundipe IE. 2017. Thermal and chemical variations of the Nigerian Benue Trough lead-zinc-barite-fluorite deposits. J Afr Earth Sci. 132:72–79. doi: 10.1016/j.jafrearsci.2017.05.004.
Okagbue CO, Uma KO. 1988. The impact of geology on the performance of a bituminous surfaced pavement – a case study from southeastern Nigeria. J Afr Earth Sci. 7 (1):257–264. doi: 10.1016/0899-5362(88)90072-3.
Ola SA. 1978. Geotechnical properties and behavior of some stabilized Nigerian laterite soil. Q J Eng Geol Hydrogeol. 11(2):145–160. doi: 10.1144/GSL.QJEG.1978.011.02.04.
Ola SA. 1980. Mineralogical properties of some Nigerian residual soils in relation with building problems. Eng Geol. 15(1–2):1–13. doi: 10.1016/0013-7952(80)90027-7.
Oladeinde SO, Magaji IJ, Ekpo AS. 2020. Assessment of climate variability trends in Nasarawa State, Nigeria. J Geogr Environ Earth Sci Int. 24(5):41–50. doi: 10.9734/jgeesi/2020/v24i530226.
Omorinbola EO. 1983. Deep weathering of interfluves in the basement complex of South-Western Nigeria: its geomorphological and geohydrological implications. Trans Inst Br Geogr. 8(3):342–360. doi: 10.2307/622049.
Orellana E, Mooney HM. 1966. Master Tables and Curves for Vertical Electrical Sounding over Layered Structures. Interciencia. p. 34.
Palacky GV. 1987. Resistivity characteristics of geologic targets. Electromagn Methods Appl Geophys. 1, Theory:1351.
Pawlik Ł, Kasprzak M. 2018. Regolith properties under trees and the biomechanical effects caused by tree root systems as recognized by electrical resistivity tomography (ERT). Geomorphology. 300:1–12. doi: 10.1016/j.geomorph.2017.10.002.
Pedron FA, Oliveira RB, Dalmolin RSD, Azevedo AC, Kilca RV. 2015. Boundary between soil and saprolite in Alisols in the south of Brazil. Rev Bras Ciênc Solo. 39 (3):643–653. doi: 10.1590/01000683rbcs20140229.
Petry TM, Little DN. 2002. Review of Stabilization of Clays and expansive soils in pavements and lightly loaded structures–history, practice, and future. J Mater Civ

Eng. 14(6):447–460. doi: 10.1061/(ASCE)0899-1561(2002)14:6(447).

Rasul JM, Burrow MPN, Ghataora GS. 2016. Consideration of the deterioration of stabilised subgrade soils in analytical road pavement design. Transp Geotech. 9:96–109. doi: 10.1016/j.trgeo.2016.08.002.

Reynolds JM. 1998. An introduction to applied and environmental geophysics. 2nd ed. Hoboken: Wiley.

Romero-Ruiz A, Linde N, Keller T, Or D. 2019. A review of geophysical methods for soil structure characterization. Rev Geophys. 56(4):672–697. doi: 10.1029/2018RG000611.

Smaida A, Mekerta B, Gueddouda MK. 2021. Physico-mechanical stabilization of a high swelling clay. Constr Build Mater. 289:123197. doi: 10.1016/j.conbuildmat.2021.123197.

Smith RB. 1988. Capacité portante d'une argile tertiaire et conséquences sur la conception de la chaussée. Bull Int Assoc Eng Geol. 37(1):137–141. doi: 10.1007/BF02590380.

Taylor GM, Eggleton RA. 2001. Regolith geology and geomorphology. Chichester, UK; New York, NY: J. Wiley.

Tukur A, Samaila NK, Grimes ST, Kariya II, Chaanda MS. 2015. Two member subdivision of the Bima Sandstone, upper Benue Trough, Nigeria: based on sedimentological data. J Afr Earth Sci. 104:140–158. doi: 10.1016/j.jafrearsci.2014.10.015.

Vaiana R, Oliviero Rossi C, Perri G. 2021. An eco-sustainable stabilization of clayey road subgrades by lignin treatment: an overview and a Comparative Experimental Investigation. Appl Sci. 11(24):11720. doi: 10.3390/app112411720.

Vander-Velpen BPA. 1988. Resistivity Depth Sounding Interpretation Software WinResist Version 1.0. M.Sc. Research Project, ITC, Delft, Netherland.

Wright EP. 1992. The hydrogeology of crystalline basement aquifers in Africa. Geol Soc London, Spec Publ. 66(1):1–27. doi: 10.1144/GSL.SP.1992.066.01.01.

Wright JB. 1981. Review of the origin and evolution of the Benue Trough in Nigeria. Earth Evolution Sci. 2:98–103.

Wright JB, Hastings DA, Jones WB, Williams HR. 1985. Geology and mineral resources of West Africa. London: George Allen and Unwin; p. 187.

Zohdy AA, Eaton CP, Mabey DR. 1974. Application of surface geophysics to ground-water investigations. Techniques of water-resources investigations 02-D1 USGS numbered series. doi: 10.3133/twri02D1.